Eur. Phys. J. C (2023) 83:233
https://doi.org/10.1140/epjc/s10052-023-11389-y

THE EUROPEAN PHYSICAL JOURNAL C

Regular Article - Theoretical Physics

Shielding of Penrose superradiance in optical black holes

Hongbin Zhang, Baocheng Zhang[a]

School of Mathematics and Physics, China University of Geosciences, Wuhan 430074, China

Received: 6 September 2022 / Accepted: 8 March 2023 / Published online: 21 March 2023

Abstract We investigate the effect of superradiance shielding for the analogue rotating black holes simulated by optical vortices by calculating the radial motion of massless particles in such spacetime background. We add the conditions $E < L\Omega_{r_e}$ and $L > 0$ to judge the classically forbidden region of superradiance. It is found that the superradiance forbidden region exists near the static limit inside the ergosphere, which will limit the classical Penrose process for the particles with some specific energies and angular momenta. Once these particles satisfying the superradiance conditions are measured at the outside of the ergosphere, this shows that the Penrose process can be quantum.

1 Introduction

The superradiance of rotating black holes was proposed [1] firstly by Penrose in the year of 1971. This can be used to extract the rotational energy of a rotating black hole in such a way that an object is emitted into the ergosphere where it is split into two pieces, in which one has negative energy and the other one can escape from the ergosphere with a positive energy gain. Furthermore, Zel'dovich [2] gave the conditions for the existence of rotational superradiance,

$$\omega < n\Omega. \tag{1}$$

where Ω is the angular velocity of the rotating black holes, ω is the angular frequency of the incident wave, and n is the wave winding number concerning the rotation axis. The superradiance can occur for the classical or quantum waves. However, radiation screening [3] for the particles with certain energies and angular momenta exists inside and outside the ergosphere for the Kerr spacetime [4] and Kerr-Newman spacetime [5], which restricts the motion of the classical particles in the ergosphere and so restricts the occurrence of classical Penrose process. For these restricted particles, the Penrose superradiance can occur by the quantum tunneling. These particles can be Hawking radiations from the event horizon, and can also be that emitted into the ergosphere from the outside [4].

In the past several years, the Penrose superradiance was studied in the analogue rotating black holes [6–10]. The concept of the analogue black holes was put forward initially in 1981 [11], based on the relation between the motion of sound waves in a convergent fluid flow and the motion of a scalar field in the background of Schwarzschild spacetime, and the analog horizon is defined by equating the velocity of the fluid with the local sound velocity in this fluid. The analogue Hawking radiation can be emitted from the analogue horizon, which has been studied in many different physical systems [12–18]. Besides simulating the Schwarzschild black holes, rotating black holes were also simulated using the physical systems [19], and some related phenomena such as superradiance [8], black-hole bombs [20], and scalar clouds [21] were investigated. In this paper, we focus on the superradiance of analogue rotating black holes, which could be measured experimentally [22–24] in some physical systems. It is pointed out that there will be no superradiance when the angular momentum is negative in the optical systems [23,24]. In this paper, we aim to explore whether the radiation shielding regions exist under the background of analogue rotating black holes simulated by the optical vortices and their influence on the Penrose superradiance.

The paper is organized as follows. In Sect. 2, we review how the metric of the analogue black holes is derived from the nonlinear Schrödinger equation and investigate the radiation shielding regions for the analogue rotating black holes. In Sect. 3, we use the conditions for the occurrence of superradiance to discuss the superradiance forbidden regions in the optical rotating black holes. Then, we study the turning (boundary) points of the classically forbidden region using an experimentally generated analogue rotating spacetime with

[a] e-mail: zhangbaocheng@cug.edu.cn (corresponding author)

a static limit but without an event horizon in Sect. 4. We also calculate the probability of the classically forbidden particle tunneling through the ergosphere. Finally, we give the conclusion in Sect. 5.

2 Radiation shielding

In order to investigate the radiation shielding phenomenon under the background of analogue gravity, we first introduce how the metric of the analogue black holes is obtained in the physical system of optical vortices. Start with the nonlinear Schrödinger equation (NLSE) [25] in the paraxial approximation, which governs the evolution of the electric field $\epsilon(x, y, z)$ of the vortex beam as,

$$\partial_z \epsilon = \frac{i}{2k}\nabla_\perp^2 \epsilon - i\frac{kn_2}{n_0}\epsilon|\epsilon|^2, \tag{2}$$

where z is the propagation direction, $k = (2\pi n_0)/\lambda$ is wave number along the z-direction, n_0 is the linear refractive index, and n_2 is the nonlinearity coefficient. In this equation, $z = c\tilde{t}/n_0$ is equivalent to time due to the constant light speed. The first term on the right-hand side describes the diffraction effect, and the second term describes the self-defocusing effects. If the electric field is expressed as $\epsilon = \sqrt{\rho_0}e^{i\phi}$, the NLSE becomes the continuity and Euler equations,

$$\partial_{\tilde{t}}\rho + \nabla\cdot(\rho\mathbf{v}) = 0, \tag{3}$$

$$\partial_{\tilde{t}}\psi + \frac{1}{2}v^2 + \frac{c^2 n_2}{n_0^3}\rho - \frac{c^2}{2k^2 n_0^2}\frac{\nabla^2\rho^{1/2}}{\rho^{1/2}} = 0, \tag{4}$$

where c is the speed of light, the optical intensity ρ corresponds to the fluid density, $v = \frac{c}{kn_0}\nabla\phi \equiv \nabla\psi$ is the fluid velocity, and the third term is the quantum pressure which is usually ignored in the linearized process for the derivation of the analogue metric. Linearizing these equations with $\rho = \rho_0 + \epsilon\rho_1$ and $\psi = \psi_0 + \epsilon\psi_1$, it is obtained that $(\frac{\rho_0}{c_s})^2(-\partial_t^2\psi_1 - \partial_t\delta_{ij}v_j\partial_j\psi_1 + c_s^2\partial_i\delta_{ij}\partial_j\psi_1 - \partial_i\delta_{ij}v_j\partial_t\psi_1 - \partial_i v_i\partial_j v_j\psi_1) = 0$ where $c_s^2 = c^2 n_2\rho_0/n_0^3$ is the local speed of sound and $i, j = 1, 2$. Rewrite the equation with the form, $\nabla^2\psi_1 = \left(1/\sqrt{-g}\right)\partial_\mu\left(\sqrt{-g}g^{\mu\nu}\partial_\nu\psi_1\right)$, one can obtain the metric as [26],

$$ds^2 = \left(\frac{\rho_0}{c_s}\right)^2\Big[-(c_s^2 - v_t^2)d\tilde{t}^2 - 2v_r dr d\tilde{t} \\ -2v_\theta r d\tilde{\theta}d\tilde{t} + dr^2 + (rd\tilde{\theta})^2\Big], \tag{5}$$

where $v_r = \partial_r\psi_0$, $v_\theta = \frac{1}{r}\partial_{\tilde{\theta}}\psi_0$ are the radial and tangential velocity components, and $v_t^2 = v_r^2 + v_\theta^2$ is the total velocity.

Making the time and angle transformations, $dt = d\tilde{t} + \frac{|v_r|}{(c_s^2 - v_r^2)}dr$, and $d\theta = d\tilde{\theta} + \frac{|v_r|v_\theta}{r(c_s^2 - v_r^2)}dr$, the analogue metric (5) becomes

$$ds^2 = \left(\frac{\rho_0}{c_s}\right)^2\Big[-(c_s^2 - v_t^2)dt^2 + \frac{c_s^2}{c_s^2 - v_r^2}dr^2 \\ +(rd\theta)^2 - 2v_\theta r d\theta dt\Big]. \tag{6}$$

It is similar to the Kerr metric in general relativity, and has the event horizon when $c_s = v_r$ and the static limit when $c_s = v_t$.

Such analogue metric has been realized by the optical vortex as given in Ref. [28] and the superradiance was studied in Ref. [29]. In this paper, we take the same parameters as in Ref. [29] to analyze the screening effect of the analogue spacetime. Take the electric field $\epsilon = \sqrt{\rho_0}exp(im\theta - 2i\pi\sqrt{\frac{r}{r_0}})$ where ρ_0 is a constant optical intensity, and $r_0 = 100\,\mu$m is an experimental parameter to form the optical black hole. $v_r = -\frac{c\pi}{kn_0\sqrt{r_0 r}}$, $v_\theta = \frac{cm}{kn_0 r}$, and $c_s = \sqrt{\frac{c^2 n_2\rho_0}{n_0^3}}$ are the radial, angular, and sound velocities, respectively. Moreover, the refractive index change takes $n_2\rho_0 = 2\times 10^{-6}$ which gives the sound velocity as $c_s = \sqrt{18}\times 10^5$ m/s. Other parameters take $\xi = \frac{c\pi}{kn_0 c_s} = 275\,\mu$m, $v_\theta = \frac{m\xi c_s}{\pi r}$, and $v_r = -\frac{\xi c_s}{\sqrt{r_0 r}}$. Thus, the event horizon of the optical black hole locates at $r_e \approx 756\,\mu$m, and the static limit at $r_s \approx 893\,\mu$m, with the topological charge $m = 4$ of the vortex beam. With these expressions in mind, the contravariant form of the analogue metric (6) can be written as

$$\mathbf{g}^{\mu\nu} = \begin{pmatrix} \frac{1}{\frac{\xi^2}{r_0 r}-1} & 0 & \frac{\frac{m\xi}{\pi r}}{r\left(\frac{\xi^2}{r_0 r}-1\right)} \\ 0 & 1-\frac{\xi^2}{r_0 r} & 0 \\ \frac{\frac{m\xi}{\pi r}}{r\left(\frac{\xi^2}{r_0 r}-1\right)} & 0 & \frac{-1+\frac{\xi^2}{r_0 r}+\left(\frac{m\xi}{\pi r}\right)^2}{r^2\left(\frac{\xi^2}{r_0 r}-1\right)} \end{pmatrix}. \tag{7}$$

In the following, we will calculate the equations of motion for particles moving in the analogue spacetime following the method by Chandrasekhar for the geodesic motion in the spacetime of Kerr black holes [30]. Considering a particle with the action S moving freely in the spacetime described with the metric (6), the Hamilton–Jacobi (HJ) equation is given as

$$2\frac{\partial S}{\partial\tau} = g^{\mu\nu}\frac{\partial S}{\partial x^\mu}\frac{\partial S}{\partial x^\nu}, \tag{8}$$

where τ is the proper time of the particle. Assuming the energy and the angular momentum of the particle are constant E and L, the action can be expressed as

$$S = -\frac{1}{2}\delta\tau - Et + L\theta + S_r(r), \tag{9}$$

where δ is a constant and determines whether the motion equation of the particle describes a time-like geodesic ($\delta > 0$) or a light-like geodesic ($\delta = 0$). Substituting metric tensor $\mathbf{g}^{\mu\nu}$ (7) and the action (9) into the HJ equation, we have

$$r^2\left(\frac{\xi^2}{r_0 r}-1\right)^2\left(\frac{\partial S_r(r)}{\partial r}\right)^2 = r^2E^2 + r^2\left(\frac{\xi^2}{r_0 r}-1\right)\delta + \left(-1+\frac{\xi^2}{r_0 r}+\left(\frac{m\xi}{\pi r}\right)^2\right) \times L^2 - \frac{2m\xi EL}{\pi}. \tag{10}$$

Integrating the Eq. (10), we obtain

$$S_r(r) = \int^r \frac{\sqrt{V_{eff}}}{r\left(\frac{\xi^2}{r_0 r}-1\right)}dr, \tag{11}$$

where the effective potential is expressed with the form

$$V_{eff} = r^2E^2 + r^2\left(\frac{\xi^2}{r_0 r}-1\right)\delta + \left(-1+\frac{\xi^2}{r_0 r}+\left(\frac{m\xi}{\pi r}\right)^2\right)L^2 - \frac{2m\xi EL}{\pi}. \tag{12}$$

With the expression of $S_r(r)$ in the action (9), we can obtain the equations of motion of the particle as

$$r\frac{dr}{d\tau} = \sqrt{V_{eff}}, \tag{13}$$

$$r\frac{dt}{d\tau} = \frac{1}{r\left(\frac{\xi^2}{r_0 r}-1\right)}\left(r^2E - \frac{m\xi L}{\pi}\right), \tag{14}$$

$$r\frac{d\theta}{d\tau} = \frac{1}{r\left(\frac{\xi^2}{r_0 r}-1\right)} \times \left(\frac{m\xi E}{\pi} - \left(-1+\frac{\xi^2}{r_0 r}+\left(\frac{m\xi}{\pi r}\right)^2\right)L\right). \tag{15}$$

These equations of motion are derived from the principle of the least action, $\frac{\partial S}{\partial \delta} = 0$, $\frac{\partial S}{\partial E} = 0$, $\frac{\partial S}{\partial L} = 0$, respectively. Under the spacetime background of optical black holes with the metric (6), we consider the massless particles which is a vortex beam emitted into the spacetime generated by another vortex beam, and their equations of motion can be derived by taking $\delta = 0$.

Note that $\frac{1}{2}\left(\frac{dr}{d\tau}\right)^2$ has the meaning of kinetic energy, so the negative effective potential makes no sense since the velocity $\frac{dr}{d\tau}$ has to be the complex value. This means that $\frac{dr}{d\tau}$ must be real in the calculation. However, the effective potential (12) can be negative for some physically allowable values of the energy E and angular momentum L under the real black-hole spacetime background. The region in which the effective potential is negative is called the classically forbidden region [3,4].

Now, we analyze whether the classically forbidden region exists under the analogue spacetime background. Fixed the angular momentum of the particle, and thus, the effective potential can be expressed as a function of E,

$$V_E = r^2E^2 - 2\frac{m\xi EL}{\pi} + \left(-1+\frac{\xi^2}{r_0 r}+\left(\frac{m\xi}{\pi r}\right)^2\right)L^2. \tag{16}$$

It is not hard to get the negative V_E which is derived between the two roots due to the quadratic term of the effective potential being positive. The classically forbidden region for values of E lies between the two roots,

$$E_\pm = \frac{m\xi L}{\pi r^2}\left(1 \pm \sqrt{1 - \frac{\frac{\xi^2}{r_0 r}+\left(\frac{m\xi}{\pi r}\right)^2-1}{\left(\frac{m\xi}{\pi r}\right)^2}}\right). \tag{17}$$

Figure 1 presents the classically forbidden region in which the radial motion of the particles is restricted. In particular, the motion for the particles within the energy range (E_-, E_+) are constrained between the blue and orange surfaces. This shows that the classically forbidden region exists for the analogue black-hole spacetime. It is also noted in Fig. 1 that the forbidden region of energy will widen when the angular momentum increases. We also present the energy forbidden region at the static limit of the analogue rotating black holes

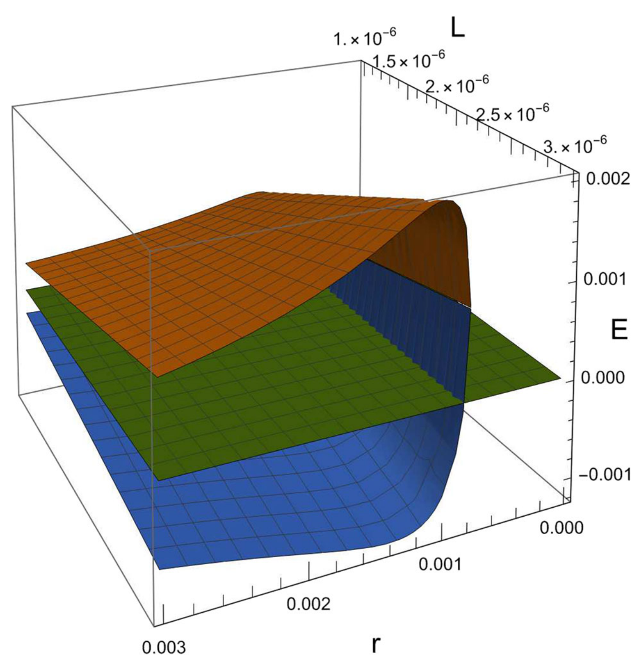

Fig. 1 Energy as the function of r and L. It indicates that the screening of Hawking radiation with certain values of energy and angular momentum between blue and orange surfaces

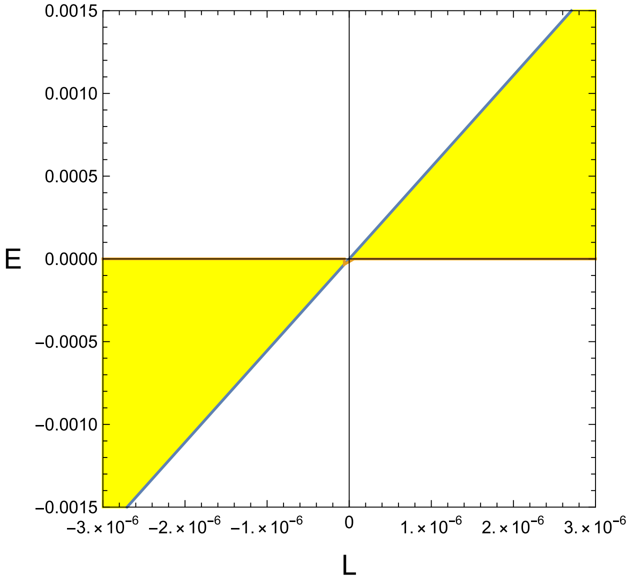

Fig. 2 Energy as a function of L. The shielding region for particles with energies and angular momenta at the static limit is marked with the yellow color

in Fig. 2. The results are similar to that in the Kerr black holes [4], which means that the optical black hole indeed can simulate the properties of the Kerr black holes. In what follows, we will focus on the shielding of Penrose superradiance with an addition of the superradiance conditions in our consideration.

3 Penrose superradiance shielding

The optical black holes have the classically forbidden region, so shielding of Penrose superradiance might cause the absence of Penrose superradiance for the optical black holes. At first, we obtain the condition for the occurrence of superradiance using the metric (6) of optical black holes. Transforming Eq. (10) using the relation $\frac{d}{dr} = \frac{1}{r\left(1-\frac{\xi^2}{r_0 r}\right)}\frac{d}{ds}$, we get

$$\left(\frac{\partial S_r}{\partial s}\right)^2 = r^2E^2 + r^2\left(\frac{\xi^2}{r_0 r}-1\right)\delta + \left(-1+\frac{\xi^2}{r_0 r}+\left(\frac{m\xi}{\pi r}\right)^2\right)L^2 - \frac{2m\xi EL}{\pi}. \tag{18}$$

Taking the radial wave function $\psi = \exp(iS_r)$, the one-dimensional Schrödinger equation is gotten as

$$\frac{d^2\psi}{ds^2} + V_{eff}\psi = 0. \tag{19}$$

Then transform back to the coordinate system of r, and the similar radial Teukolsky equation [31,32] is obtained as

$$r\left(1-\frac{\xi^2}{r_0 r}\right)\frac{d}{dr}\left[r\left(1-\frac{\xi^2}{r_0 r}\right)\frac{d\psi}{dr}\right] + V_{eff}\psi = 0. \tag{20}$$

Transforming the radial coordinate r into the tortoise coordinate r^* by $r^* = r+\frac{\xi^2}{r_0}ln\left(r-\frac{\xi^2}{r_0}\right)$ and taking the new form of radial wave function $\psi^* = \sqrt{r}\psi$, we get a linear second-order differential equation

$$\frac{d^2\psi^*}{dr^{*2}} + V'_{eff}\psi^* = 0, \tag{21}$$

where $V'_{eff} = \frac{1}{4r^2}\left(\frac{dr}{dr^*}\right)^2 - \frac{1}{r^2}\left(L^2+\frac{\xi^2}{2rr_0}\right)\left(\frac{dr}{dr^*}\right) + (E - L\frac{m\xi}{\pi r^2})^2$. It is not hard to obtain the asymptotic solution $\psi^* = e^{iEr^*} + Re^{-iEr^*}$ for $r^* \to +\infty$, $r \to +\infty$, $\frac{dr}{dr^*} \to 1$, and another asymptotic solution $\psi^* = Te^{i\left(E-L\frac{m\xi}{\pi r_e^2}\right)r^*}$ for $r^* \to -\infty$ $r \to r_+$, $\frac{dr}{dr^*} \to 0$, where R is the reflection coefficient and T is the transmission coefficient. Then we can equate the Woronskian of the two asymptotic solutions to get the relation

$$|R|^2 = 1 - \frac{E-L\Omega_{r_e}}{E}|T|^2, \tag{22}$$

where $\Omega_{r_e} = \frac{m\xi}{\pi r_e^2}$ is the angular velocity at the horizon. When $|R|^2 > 1$, the superradiance occurs, which leads to the superradiance condition

$$E < L\Omega_{r_e}. \tag{23}$$

This is consistent with the result in Eq. (1) by Zel'dovich when taking $E = \hbar\omega$ and $L = \hbar n$ for a quantum energy and angular momentum of the vortex beam, respectively.

In order to incorporate the superradiance condition (23) in the following discussions about the classically forbidden region. We rewrite the effective potential (16) as a function of $\frac{E}{L}$,

$$V_{\frac{E}{L}} = r^2\left(\frac{E}{L}\right)^2 - 2\frac{m\xi}{\pi}\left(\frac{E}{L}\right) + \left(-1+\frac{\xi^2}{r_0 r}+\left(\frac{m\xi}{\pi r}\right)^2\right). \tag{24}$$

Using superradiance condition (23), we can gain the classically forbidden region of superradiance when $V_{\frac{E}{L}} < 0$. Solving the equation $V_{\frac{E}{L}} = 0$, we obtain two roots,

$$\left(\frac{E}{L}\right)_\pm = \frac{m\xi}{\pi r^2}\left(1\pm\sqrt{1-\frac{\frac{\xi^2}{r_0 r}+\left(\frac{m\xi}{\pi r}\right)^2-1}{\left(\frac{m\xi}{\pi r}\right)^2}}\right), \tag{25}$$

which gives the superradiance forbidden region between these two roots. The upper panel of Fig. 3 presents the forbidden region under the green line Ω_{r_e} but above the red

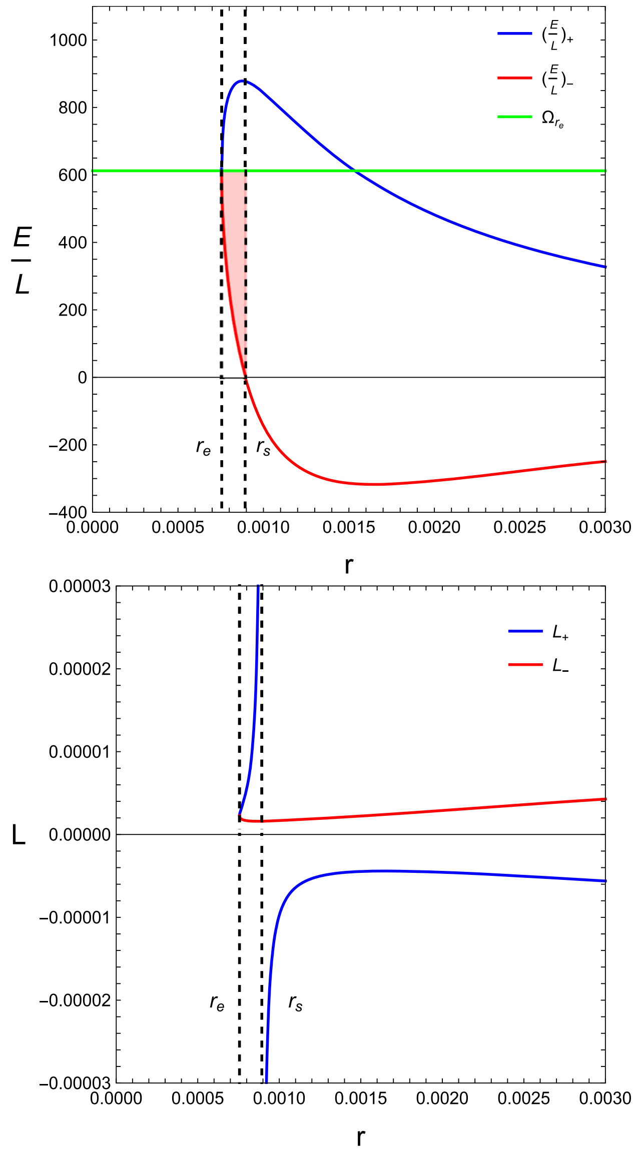

Fig. 3 $\frac{E}{L}$ and L as the function of r for the upper and lower panel, respectively. The forbidden regions in two plots are presented with the event horizon at $r_e \approx 756\,\mu\text{m}$, the static limit at $r_s \approx 893\,\mu\text{m}$, and the parameters $\xi = 275\,\mu\text{m}$, $\Omega_{r_e} = \frac{v_\theta}{r_e} = 612.22$

line. We also mark the superradiance forbidden region in the ergosphere with the red shadow. It is noted that there is also the allowable region for the superradiance in the ergosphere below the red line, and the classically forbidden region is larger than the superradiance forbidden region between the blue line and the green line in the ergosphere. Thus, we give the classically forbidden region inside the ergosphere that the particles with a certain energy and angular momentum in the red region are shielded. In particular, it requires not only the condition (23) but also $n > 0$ which is a supplementary condition for the occurrence of superradiance, equivalent to $L > 0$ [21]. In order to present the influence of the angular momentum further, the effective potential (16) can be reexpressed as a function of L,

$$V_L = \left(-1 + \frac{\xi^2}{r_0 r} + \left(\frac{m\xi}{\pi r}\right)^2\right) L^2 - 2\frac{m\xi E L}{\pi} + r^2 E^2. \tag{26}$$

Solving the equation $V_L = 0$, two roots are obtained,

$$L_\pm = \frac{\frac{m\xi E}{\pi}}{-1 + \frac{\xi^2}{r_0 r} + \left(\frac{m\xi}{\pi r}\right)^2} \left(1 \pm \sqrt{1 - \frac{-1 + \frac{\xi^2}{r_0 r} + \left(\frac{m\xi}{\pi r}\right)^2}{\left(\frac{m\xi}{\pi r}\right)^2}}\right). \tag{27}$$

Since the quadratic term of the Eq. (26) is negative in the ergosphere and positive at the outside of the static limit, the classically forbidden region of angular momentum lies between the two roots in the ergosphere and outside the range between two roots at the outside of the static limit. The lower panel of Fig. 3 presents the classically forbidden region for the angular momentum. It is noted that there is also the allowable region in the ergosphere for some specific angular momenta above the blue line, but the forbidden region is near the static limit, which means that the outer particles are hard to enter the ergosphere and the Hawking radiation from the event horizon is hard to leave the ergosphere for the higher angular momentum. Meanwhile, it is also noted that there is no shielding of the Penrose superradiance for $L < 0$ since the superradiance doesn't occur in this region. So we get an angular momentum forbidden region between L_+ and L_- inside the ergosphere.

Finally, we have to point out that it is not possible to judge whether superradiance shielding occurs in the ergosphere only based on the negative effective potential, and it also requires to consider the superradiance conditions $E < L\Omega_{r_e}$ and $L > 0$. From Eq. (27), $L_\pm$ are proportional to the energy E, which means that the smaller the energy, the larger the range of forbidden region. Thus, the classical particles are harder to realize the Penross process. Quantum tunneling is necessary for the occurrence of Penrose superradiance with low energy. In the following section, we will discuss this using a model related to the recent experiment for Penrose superradiance using the optical vortices.

4 Quantum tunneling

As in recent numerical simulation [23] and experimental measurement [24] about Penrose superradiance, the analogue metric for optical black holes is written simply as

$$ds^2 \propto -(c_s^2 - v_\theta^2)dt^2 + dr^2 + (rd\theta)^2 - 2v_\theta r d\theta dt. \tag{28}$$

where c_s and v_θ have the same forms as in the last section. In Refs. [23,24], two laser beams were applied to simulate the superradiance phenomena, in which the pump beam was used to form the background spacetime as given in metric (28) and the signal beam was transformed into an amplified output beam under the condition that an idler beam with the negative-frequency modes trapped within the ergoregion was generated. It is noted that the optical field of the pump beam only had an angular phase which was used to define the angular velocity and the static limit could be obtained by making the angular velocity be equal to the sound speed, but no radial velocity exists which indicates the absence of the event horizon, as presented in the metric (28). This is convenient to study the phenomena derived from the existence of the static limit, which captures the negative-energy particles and causes the Penrose superradiance.

Using the same method as in the last section, we obtain the geodesic equations

$$r^2\left(\frac{dr}{d\tau}\right)^2 = r^2E^2 - \delta r^2 - \frac{2m\xi EL}{\pi} + \left(\left(\frac{m\xi}{\pi r}\right)^2 - 1\right)L^2, \tag{29}$$

$$r^2\frac{d\theta}{d\tau} = -\frac{m\xi E}{\pi} + L\left(\left(\frac{m\xi}{\pi r}\right)^2 - 1\right), \tag{30}$$

$$r^2\frac{dt}{d\tau} = -Er^2 + \frac{m\xi L}{\pi}, \tag{31}$$

and the effective potential

$$V_{eff} = r^2E^2 - \delta r^2 - \frac{2m\xi EL}{\pi} + \left(\left(\frac{m\xi}{\pi r}\right)^2 - 1\right)L^2. \tag{32}$$

This effective potential can be expressed as the function of $\frac{E}{L}$, and solving $V_{eff}\left(\frac{E}{L}\right) = 0$, we get two roots

$$\left(\frac{E}{L}\right)_\pm = \frac{m\xi}{\pi r^2}\left(1 \pm \sqrt{1 - \frac{\left(\frac{m\xi}{\pi r}\right)^2 - 1}{\left(\frac{m\xi}{\pi r}\right)^2}}\right) \tag{33}$$

and consider the effective potential as the function of L, and solving $V_{eff}(L) = 0$, we get two roots

$$L_\pm = \frac{\frac{m\xi E}{\pi}}{-1 + \left(\frac{m\xi}{\pi r}\right)^2}\left(1 \pm \sqrt{1 - \frac{-1 + \left(\frac{m\xi}{\pi r}\right)^2}{\left(\frac{m\xi}{\pi r}\right)^2}}\right). \tag{34}$$

By these roots, we can get the classically forbidden region for the spacetime with the metric (28).

Figure 4 presents the corresponding forbidden regions with the parameters from Ref. [24]. For example, the linear refractive index $n_0 = 1.32$, the nonlinearity coefficient $n_2 = 4.4 \times 10^{-7} cm^2/W$, the wavelength $\lambda = 532nm$, the pump power $P = 252mW$, the value of the pump waist $\omega_{bg} = 1cm$, the pump orbital angular momentum (OAM) $l = 1$, and the signal OAM $s = 2$. The pump intensity is gotten as $I = \rho_0 = P/\omega_{bg}^2$, healing length $\xi = \lambda/\sqrt{4n_0|n_2|\rho_0}$, the speed of sound $c_s = \sqrt{c^2|n_2|\rho_0/n_0^3}$, the flow speed $v_\theta = c|m|/n_0kr$, and $m = s - l$.

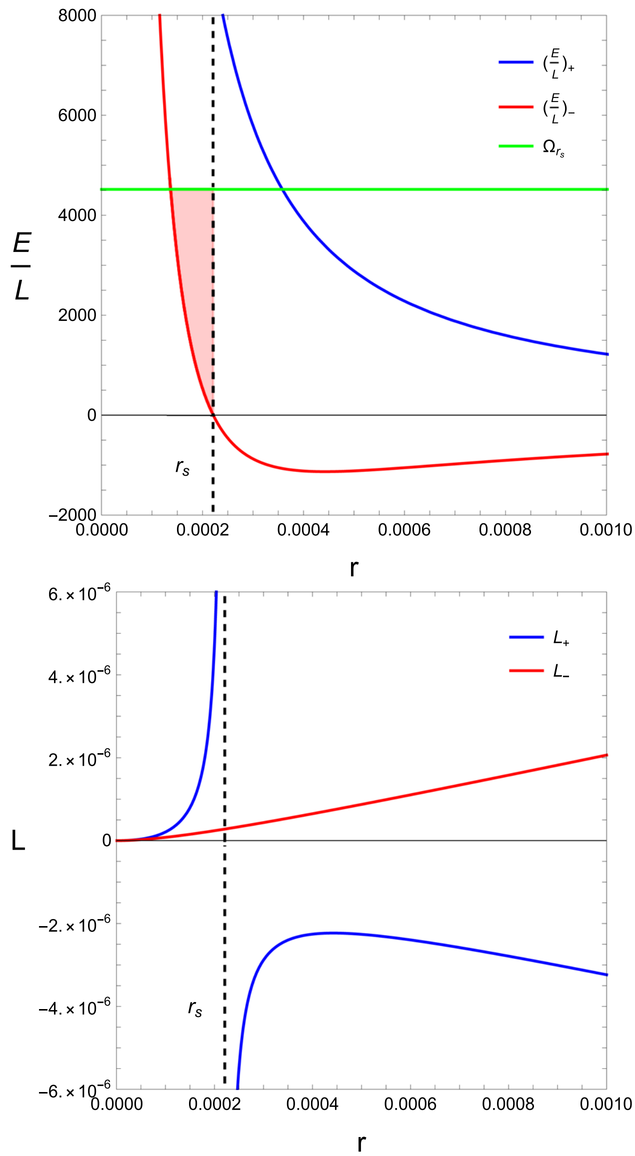

Fig. 4 $\frac{E}{L}$ and L as the function of r for the upper and lower panel, respectively. The forbidden regions in two plots are presented with the static limit at $r_s \approx 221\,\mu$m, and the parameters $\xi = 695\,\mu$m, $\Omega_{r_s} = \frac{v_\theta}{r_s} = 4518.37$

In the upper panel of Fig. 4, the superradiance forbidden region inside the ergosphere is given with the red shadow, which is near the static limit. The angular momentum forbidden region is presented in the lower panel of Fig. 4, and the forbidden region inside the ergosphere is also near the static limit. These show that the shielding of Penrose superradiance is probable although only the static limit exists and the event horizon doesn't exist. Of course, the superradiance shielding region has to satisfy these conditions $E < L\Omega_{r_s}$ and $L > 0$, as presented in the upper panel of Fig. 4. Although there is a red forbidden region in the ergosphere, particles can tunnel across the forbidden region.

Now consider the quantum tunneling in the analogue metric (28). When $\delta = 0$, the effective potential (32) becomes

$$V_{eff} = \frac{m^2\xi^2 L^2}{\pi^2}\frac{1}{r^4} - \left(\frac{2mEL\xi}{\pi} + L^2\right)\frac{1}{r^2} + E^2. \quad (35)$$

To study the quantum tunneling, we need to know the boundary locations of the forbidden region, which can be obtained by solving $V_{eff} = 0$ for the roots of r with the fixed energy and angular momentum. Because the equation $V_{eff} = 0$ is a biquadratic equation, we can solve the roots for $x = r^2$,

$$x_{1,2} = \frac{2m\xi EL + \pi L^2}{2E^2\pi}\left(1 \pm \sqrt{1 - \frac{4E^2m^2\xi^2L^2}{\left(2m\xi EL + \pi L^2\right)^2}}\right). \quad (36)$$

x must be real, or else r will take the complex values. According to Descartes' rule of signs, when the three terms in V_{eff} have the sign $+ - +$, the equation $V_{eff} = 0$ has two positive roots for x. Thus,

$$r_1 = \sqrt{x_1}, \quad r_2 = -\sqrt{x_1}, \quad r_3 = \sqrt{x_2}, \quad r_4 = -\sqrt{x_2}, \quad (37)$$

are four turning points that the forbidden region changes to the allowable region for the motion of classical particles.

The one-dimensional Schrödinger equation with potential V_{eff} is

$$\frac{d^2\psi(r)}{dr^2} = -V_{eff}\psi(r). \quad (38)$$

The particles can tunnel through the potential barrier when $V_{eff} < 0$, and the tunneling probability is proportional to Gamow factor $e^{-2\gamma}$, where

$$\gamma = \int_{r_1}^{r_3} \sqrt{-V_{eff}}dr. \quad (39)$$

The distance between the turning points r_1 and r_3 is regarded as the width of the potential barrier. The tunneling probability will decrease as the angular momentum of the particles increases or the energy of the particles decreases. So Penrose superradiance shielding in analogue black holes will reduce the particles with low energies and high angular momenta, as presented in Fig. 5.

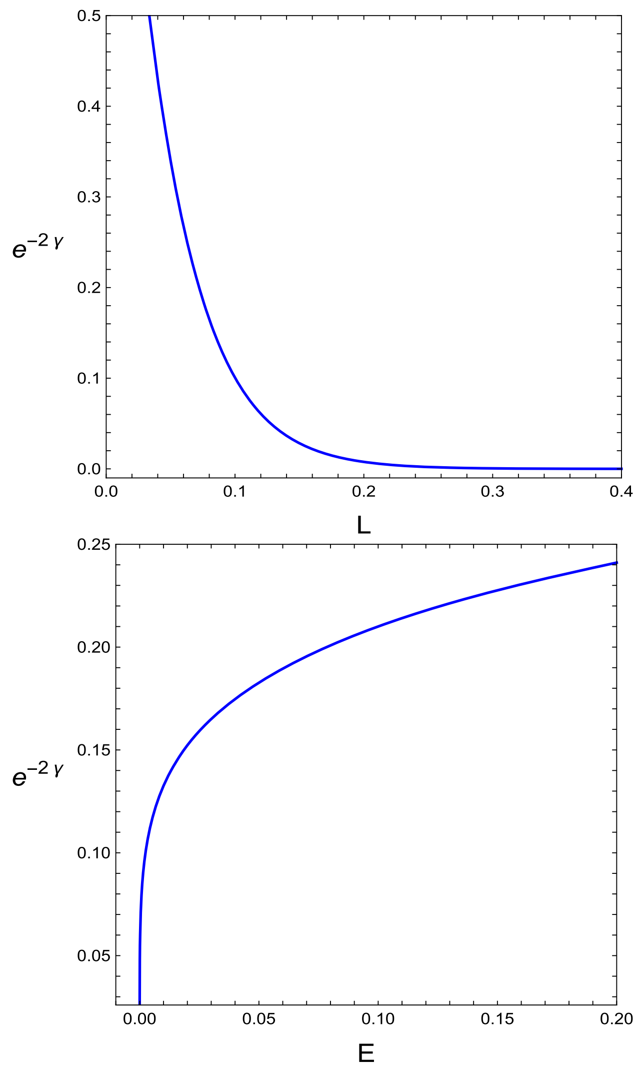

Fig. 5 Gamow factor as the function of angular momentum with the energy $E = 0.00252$ in the upper panel and as the function of energy with the angular momentum $L = 0.1$

5 Conclusion

In this paper, we investigate the radiation screening under the background of optical analogue black holes and analyze mainly the Penrose superradiance shielding for two analogue metrics, with and without the existence of the event horizon, respectively. In order to show the existence of superradiance shielding, we add the conditions for the occurrence of the superradiance to analyze the classically forbidden region. We find that the forbidden region is near the static limit for two different analogue metrics, which means that the superradiance shielding is probable for the particles with the specific energies and angular momenta. For the forbidden particles, we calculate the tunneling probability, which shows that the particles with high energies and low angular momenta are easier to tunnel through the barrier. We use the experimental parameters to make the corresponding analyses for the forbidden region and the tunneling, which is helpful to show that some superradiances with the specific energies and angular momentum can be measured by the tunneling through the static limit. Thus, these superradiances are quantum.

Acknowledgements This work is supported from Grant No. 11654001 of the National Natural Science Foundation of China (NSFC).

Data Availability Statement This manuscript has no associated data or the data will not be deposited. [Authors' comment: This paper is a purely theoretical calculation, and all relevant mathematical calculations are explicitly presented in this paper.]

Funded by SCOAP^3. SCOAP^3 supports the goals of the International Year of Basic Sciences for Sustainable Development.

References

1. R. Penrose, R.M. Floyd, Nat. Phys. Sci. **229**, 177 (1971)
2. Y.B. Zel'Dovich, Sov. J. Exp. Theor. Phys. Lett. **14**, 180 (1971)
3. E.M. Prodanov, Class. Quantum Gravity **31**, 105013 (2014)
4. E. Mc Caughey, Eur. Phys. J. C **76**, 1 (2016)
5. U.A. Gillani, K. Saifullah, Astropart. Phys. **125**, 102496 (2021)
6. S. Basak, P. Majumdar, Class. Quantum Gravity **20**, 3907 (2003)
7. S. Basak, P. Majumdar, Class. Quantum Gravity **20**, 2929 (2003)
8. A. Prain, C. Maitland, D. Faccio, F. Marino, Phys. Rev. Lett. **46**, 1351 (1981)
9. S. Patrick, Class. Quantum Gravity **38**, 095010 (2021)
10. Phys. Rev. Res. **4**, 033117 (2022)
11. W.G. Unruh, Phys. Rev. Lett. **46**, 1351 (1981)
12. S. Weinfurtner, E.W. Tedford, M.C.J. Penrice, W.G. Unruh, G.A. Lawrence, Phys. Rev. Lett. **106**, 021302 (2011)
13. H.S. Vieira, Chin. Phys. C **41**, 043105 (2017)
14. V.I. Kolobov, K. Golubkov, J.R.M. de Nova, J. Steinhauer, Nat. Phys. **17**, 362 (2021)
15. J.R.M. de Nova, K. Golubkov, V.I. Kolobov, J. Steinhauer, Nature **569**, 688 (2019)
16. A. Fabbri, R. Balbinot, Phys. Rev. Lett. **126**, 111301 (2021)
17. T.G. Philbin, C. Kuklewicz, S. Robertson, S. Hill, F. Konig, U. Leonhardt, Science **319**, 1367 (2008)
18. S.J. Robertson, J. Phys. B **45**, 163001 (2012)
19. C. Barceló, S. Liberati, M. Visser, Living Rev. Relativ. **14**, 3 (2011)
20. E. Berti, V. Cardoso, J.P.S. Lemos, Phys. Rev. D **70**, 124006 (2004)
21. M. Ciszak, F. Marino, Phys. Rev. D **103**, 045004 (2021)
22. T. Torres, S. Patrick, A. Coutant, M. Richartz, E.W. Tedford, S. Weinfurtner, Nat. Phys. **13**, 833 (2017)
23. M.C. Braidotti, D. Faccio, E.M. Wright, Phys. Rev. Lett. **125**, 193902 (2020)
24. M.C. Braidotti, R. Prizia, C. Maitland, F. Marino, A. Prain, I. Starshynov, N. Westerberg, E.M. Wright, D. Faccio, Phys. Rev. Lett. **128**, 013901 (2022)
25. R.W. Boyd, *Nonlinear Optics*, 2nd edn. (Academic Press, New York, 2002)
26. F. Marino, Phys. Rev. A **78**, 063804 (2008)
27. N. Cruz, C. Martinez, L. Pena, Class. Quantum Gravity **11**, 2731 (1994)
28. D. Vocke, C. Maitland, A. Prain, K.E. Wilson, F. Biancalana, E.M. Wright, F. Marino, D. Faccio, Optica **5**, 1099 (2018)
29. F. Marino, M. Ciszak, A. Ortolan, Phys. Rev. A **80**, 065802 (2009)
30. S. Chandrasekhar, *The Mathematical Theory of Black Holes* (Oxford University Press, Oxford, 1998)
31. W.H. Press, S.A. Teukolsky, Nature (London) **238**, 211 (1972)
32. S.A. Teukolsky, Astrophys. J. **185**, 635 (1973)